t$\bar{t}$ plus jets measurements

Lluïsa-Maria Mir for the ATLAS and CMS Collaborations

IFAE, Edifici Cn, UAB, E-08193 Bellaterra (Barcelona) Spain

Jet multiplicity distributions are measured in pp collisions at $\sqrt{s} = 7$ and 8 TeV with the ATLAS and CMS detectors at the LHC. The measurements are performed in the dileptonic and the lepton plus jets channels. Several QCD calculations are compared with the data.

1 Introduction

About half of the total $t\bar{t}$ events produced at the Large Hadron Collider have additional hard jets in the final state. To describe these events correctly, higher order QCD calculations, including contributions from initial and final state radiation, are required. Precise measurements of the jet multiplicity in $t\bar{t}$+jets events are useful not only to provide a test of perturbative QCD, but also because they are an important background to $t\bar{t}H$ and some SUSY final states. Finally, anomalous production of $t\bar{t}$+ jets could signal physics beyond the Standard Model (SM).

In the SM, top quarks decay most of the times to a W boson and a bottom quark. Depending on the decay mode of the W there are three different $t\bar{t}$ signatures: fully hadronic, lepton plus jets and dileptonic final states. This note includes results obtained in the lepton plus jets and the dileptonic channels with the ATLAS [1] and CMS [2] detectors. CMS uses the complete 2011 and 2012 datasets, which amount to 5 fb^{-1} and 19.6 fb^{-1} respectively, whereas ATLAS uses only the 2011 dataset, which amounts to 4.7 fb^{-1}.

2 Theoretical predictions

Data are compared with several predictions from perturbative QCD calculations. Table 1 summarizes the different simulated samples used in the analyses.

3 Dilepton channel

The dilepton channel is particularly suited to the study of $t\bar{t}$ jet multiplicity distributions as, at leading order, only two charged leptons and two b-jets are produced in the final state. Thus, any additional jet can be ascribed to higher order QCD effects. Jets are reconstructed differently in ATLAS and CMS. ATLAS forms topological clusters from energy deposits. These clusters are then used as input to the anti-k$_T$ algorithm [3] with a radius parameter of $R = 0.4$. CMS reconstructs events using a particle-flow technique, in which signals from all subdetectors are combined. Jets are reconstructed by clustering the particle-flow candidates using the anti-k$_T$ algorithm with size parameter $R = 0.5$.

Sample	ATLAS	CMS
$t\bar{t}$	Alpgen [4]+Herwig [5]	MadGraph [6]+Pythia [7]
	Alpgen+Pythia	Powheg [8]+Pythia
	Powheg+Pythia	MC@NLO [9]+Herwig
	MC@NLO+Herwig	
W+jets	Alpgen+Herwig	MadGraph+Pythia
Z+jets	Alpgen+Herwig	MadGraph+Pythia
Diboson	Herwig	MadGraph+Pythia
Single top	AcerMC [10] (t-channel)	Powheg+Pythia
	MC@NLO (all channels)	
$Z/\gamma*$		MadGraph+Pythia

Table 1: Simulated samples used in the jet multiplicity measurements.

ATLAS	CMS
Electrons: $p_T > 25$ GeV & $|\eta| < 2.47$	Electrons: $p_T > 20$ GeV & $|\eta| < 2.4$
Muons: $p_T > 20$ GeV & $|\eta| < 2.5$	Muons: $p_T > 20$ GeV & $|\eta| < 2.4$
Jets: $p_T > 25$ GeV & $|\eta| < 2.4$	Jets: $p_T > 30$ GeV & $|\eta| < 2.4$
Single lepton triggers	Dilepton triggers
Two opposite-sign leptons	At least two opposite-sign leptons
At least two jets	At least two jets
At least two identified b-jets ($\epsilon_{\text{tagging}} \approx 70\%$)	At least one identified b-jet ($\epsilon_{\text{tagging}} \approx 80 - 85\%$)
$E_T^{\text{miss}} > 40$ GeV (ee, $\mu\mu$ only)	$E_T^{\text{miss}} > 30$ (40) GeV in the 7 (8) TeV data analysis
$H_T > 130$ GeV ($e\mu$ only)	
Veto Z-boson and vector-meson regions (ee, $\mu\mu$)	Veto Z-boson and vector-meson regions (ee, $\mu\mu$)
	Use kinematic reconstruction to determine top-pair properties and identify 2 b-jets originating from decays of t-quarks

Table 2: ATLAS (7 TeV data analysis) and CMS (both 7 TeV and 8 TeV data analyses) dilepton channel event selection criteria [13–15].

The $t\bar{t}$ pairs are reconstructed requiring two isolated charged leptons, electrons or muons, at least two jets, and at least one (ATLAS) or two (CMS) candidate b-jets. Table 2 shows the details of the different event selection criteria applied in the ATLAS [13] and CMS [14, 15] analyses.

The jet multiplicity distributions show good agreement with the theoretical predictions, although the simulation predicts a slightly higher jet multiplicity than observed in 8 TeV data, as can be seen in Fig. 1.

The differential cross-section as a function of the jet multiplicity is measured from the number N_{data}^i of events in data in bin i, the number of estimated background events N_{bkg}^i, the integrated luminosity $\mathcal{L}$, the bin width Δ_x^i and a factor ϵ^i to correct for detector efficiencies and acceptances in each bin of the measurement, according to the expression

$$\frac{d\sigma_{t\bar{t}}}{dN} = \frac{N_{data}^i - N_{bkg}^i}{\Delta_x^i \epsilon^i \mathcal{L}}. \tag{1}$$
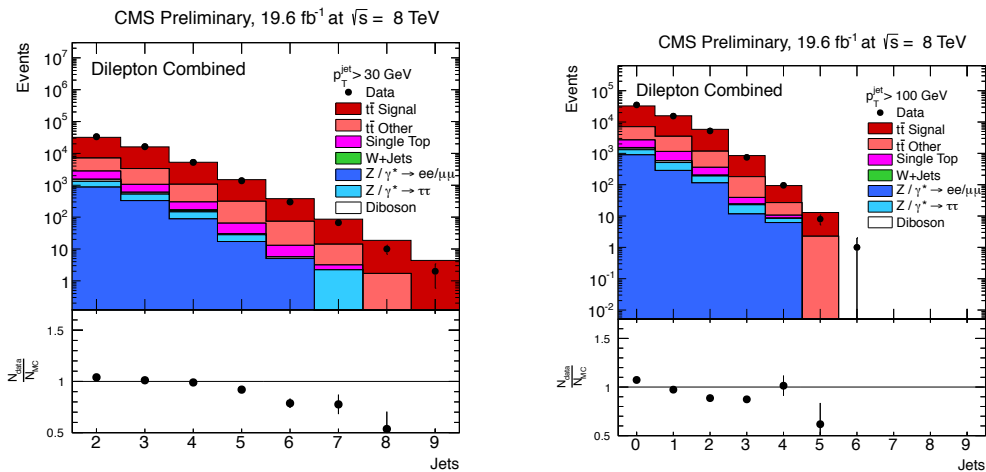
Figure 1: Reconstructed CMS jet multiplicity distribution after event selection for all jets with transverse momenta above 60 GeV (left) and 100 GeV (right) [15].

The normalised differential cross-section is derived by dividing it by the total cross-section measured in the same analysis. The advantage of using normalised cross-sections is that systematic uncertainties correlated across all bins of the measurement cancel out. The migration of events across bin boundaries and the statistical correlations among neighbouring bins caused by trigger and detector efficiencies and resolutions are corrected using a regularised unfolding method [16,17]. Several sources of systematic uncertainty have ben considered, originating both from detector effects as well as theoretical uncertainties. The dominant systematic uncertainties arise from the uncertainty of the jet energy scale as well as from model uncerainties. The total systematic uncertainty is about 3% at low jet multiplicities increasing to about 20% in the bin with at least five jets. The latter is dominated by the statistical uncertainty of the modified simulated samples.

Figure 2 shows the normalised differential cross-section as a function of the jet multiplicity for the 8 TeV CMS data sample. In general MADGRAPH and POWHEG generators interfaced with PYTHIA provide a reasonable description of the data, whereas MC@NLO interfaced with HERWIG does not generate sufficiently large jet multiplicities. The choice of larger scales leads to an improved description of the data up to high jet multiplicities. The same behaviour is observed in the 8 TeV data sample.

An alternative way to quantify the jet activity that arises from quark and gluon radiation is to determine the fraction of events that do not contain additional jets above a given threshold. The 'gap fraction' variable is defined as

$$f(Q_0) = \frac{n(Q_0)}{N}, \tag{2}$$

where N is the number of selected events and $n(Q_0)$ is the subset of those that do not contain any additional jet above a transverse momentum threshold Q_0 in a central rapidity interval. This veto can be extended beyond the leading additional jet using the alternate definition
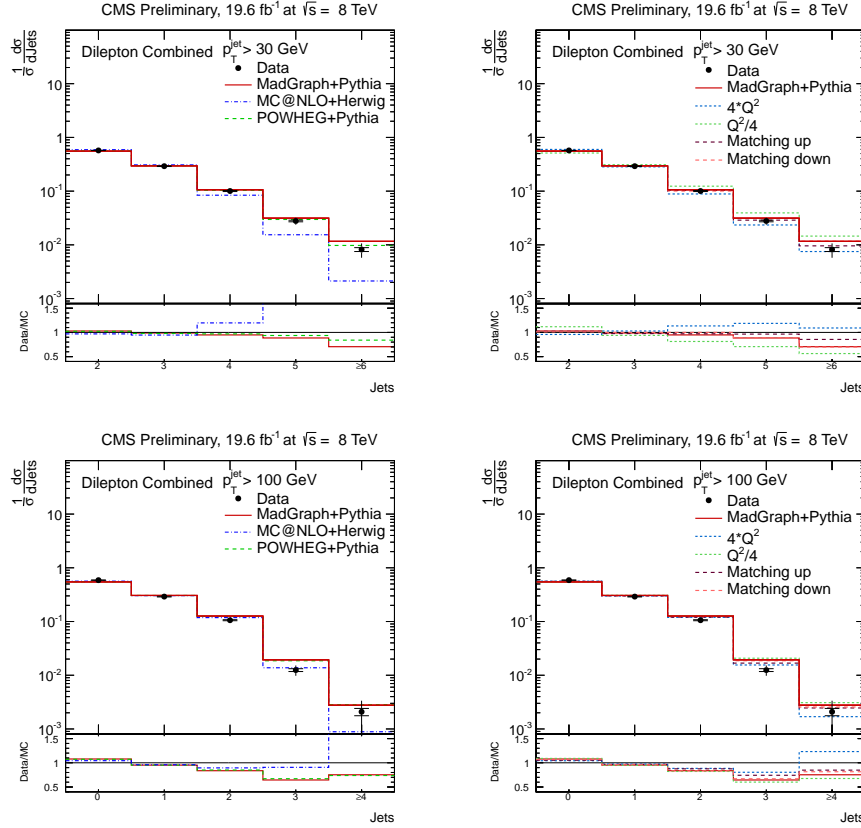
Figure 2: Normalised CMS differential cross-section as a function of the jet multiplicity for jets with $p_T > 30$ GeV (top row) and $p_T > 100$ GeV (bottom row). The figures on the left show the comparison of the data with different theoretical predictions. The figures on the right show the behaviour of the MADGRAPH generator when varying the Q^2 and matching scales [15].

$$f(Q_{sum}) = \frac{n(Q_{sum})}{N}, \tag{3}$$

where $n(Q_{sum})$ is the number of events in which the scalar transverse momentum sum of the additional jets in the rapidity interval is less than Q_{sum}. This definition is sensitive to all hard emissions accompanying the $t\bar{t}$ system.

Using 7 TeV data, ATLAS measures the gap fraction as a function of Q_0 and Q_{sum}, as shown in Figs. 3 and 4, which compare the data with several theoretical predictions in three rapidity regions. Data have been corrected for detector effects to obtain results at the particle level. Reasonable agreement is found in the full rapidity interval, but no simulation agrees in the most forward region, where too much jet activity is predicted. MC@NLO predicts too little activity in the central region as well. The fact that $f(Q_{sum})$ is lower than $f(Q_0)$ probes quark and gluon radiation beyond first emission. Only 2.05 fb^{-1} of data are used in this measurement.
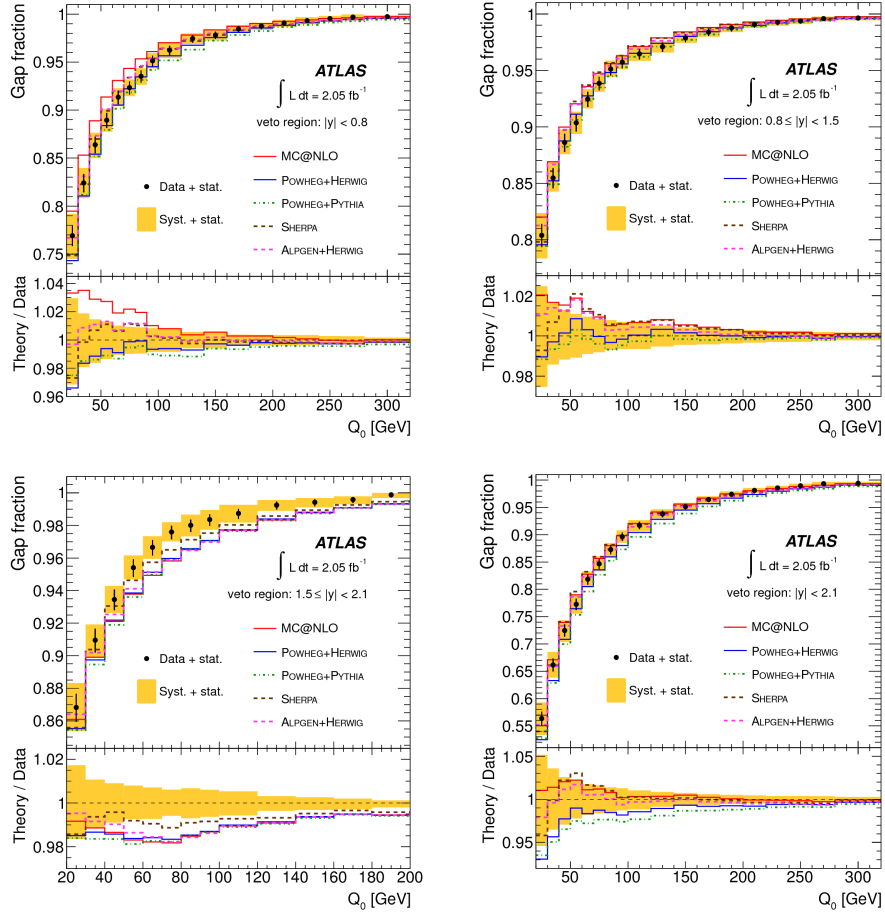
Figure 3: Measured ATLAS gap fraction as a function of Q_0 compared with several theoretical predictions in different rapidity regions [13]. The measurement is done with 7 TeV data.

CMS performs similar measurements using both 7 and 8 TeV data, and in addition studies the gap fraction for the second additional jet. In general, all generators are found to give a reasonable description of the data. Differences between MC@NLO interfaced with HERWIG and POWHEG or MADGRAPH are similar to the precision of the measurements. Increasing the Q^2 scale improves the agreement of MADGRAPH with data, while varying the matching thresholds increases the difference between data and simulation.

4   Lepton plus jets channel

The $t\bar{t}$ pairs are reconstructed in this channel requiring one isolated charged lepton, electron or muon, at least three jets, and at least one (ATLAS) or two (CMS) candidate b-jets. Jets are reconstructed using the same methods presented in Section 3. Table 3 shows the details of the
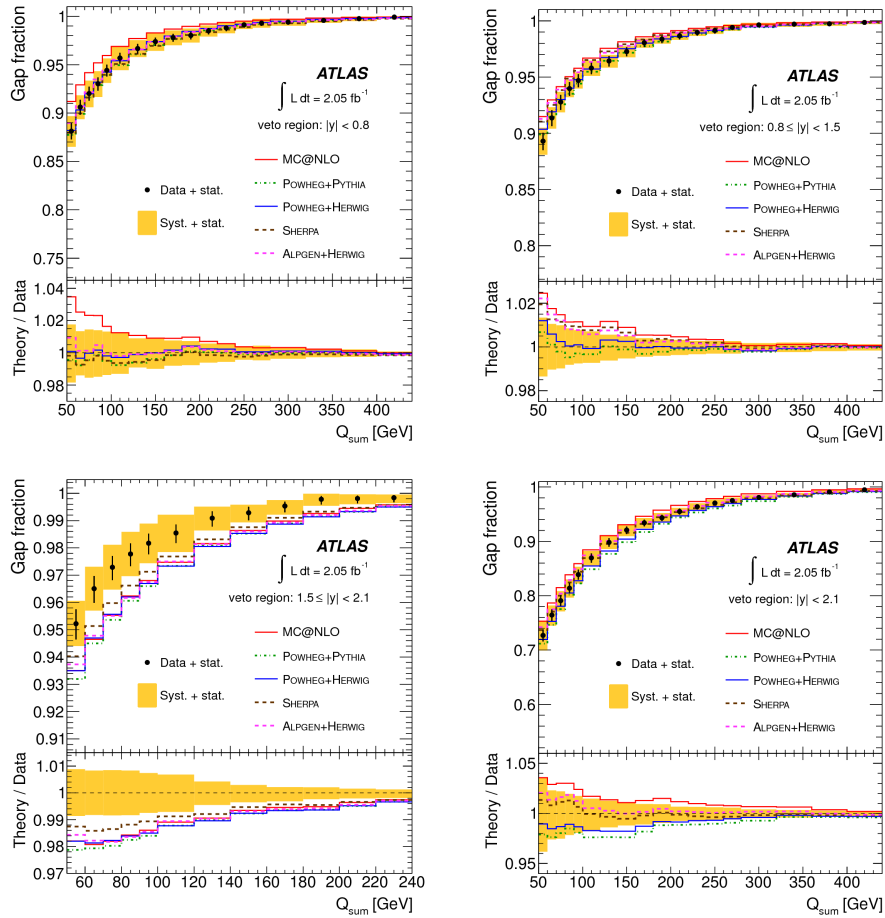
Figure 4: Measured ATLAS gap fraction as a function of Q_{sum} compared with several theoretical predictions in different rapidity regions [13]. The measurement is done with 7 TeV data.

different event selection criteria applied in the ATLAS [18] and CMS [19] analyses.

This channel suffers from more background than the dilepton one, mainly from W+jets and QCD multijet processes. The shape of the W+jets background is assumed to be well described by the simulation whereas its overall normalisation is extracted from data, using the ratio between the W^+ and W^- production cross-sections, whose theoretical prediction is known with a precision of few percent. The normalisation is obtained separately for $W + 3$ jet, $W + 4$ jet and $W+ \geq 5$ jet events. ATLAS evaluates the QCD multijet background from data using a matrix method. CMS exploits the fact that leptons from QCD multijet events are expected to be less isolated than leptons in other processes, and obtains a reasonably pure sample of QCD multijet events by inverting the selection criteria placed on the lepton relative isolation. Contributions from other processes are obtained from simulation. Fig. 5 shows the jet multiplicity distributions for the CMS 7 TeV data sample.

ATLAS corrects the jet multiplicity spectra back to the particle level by accounting for

ATLAS	CMS
Electrons: $p_T > 25$ GeV & $\|\eta\| < 2.47$	Electrons: $p_T > 30$ GeV & $\|\eta\| < 2.5$
Muons: $p_T > 25$ GeV & $\|\eta\| < 2.5$	Muons: $p_T > 30$ GeV & $\|\eta\| < 2.1$
Jets: $p_T > 25$ GeV & $\|\eta\| < 2.5$	Jets: $p_T > 35$ GeV & $\|\eta\| < 2.4$
Single lepton triggers	Single muon and single electron plus 3 jets triggers
Exactly one isolated lepton matching trigger	Exactly one isolated lepton
Veto events with other leptons with $p_T > 15$ GeV	
At least three jets	At least three jets
At least one identified b-jet ($\epsilon_{\text{tagging}} \approx 70\%$)	At least two identified b-jets ($\epsilon_{\text{tagging}} \approx 80-85\%$)
$E_T^{\text{miss}} > 30$ GeV	
$m_T(W) > 35$ GeV	

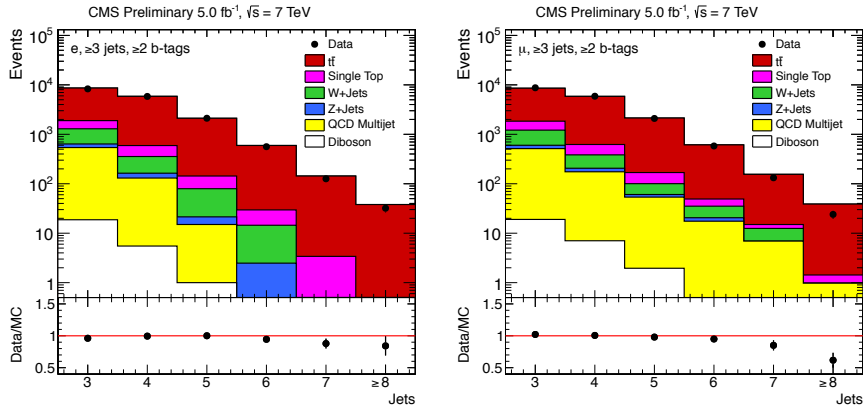Table 3: Lepton plus jets channel event selection criteria [18, 19].

Figure 5: Reconstructed CMS jet multiplicity distribution after event selection for all jets in the e+jets (left) and μ+jets (right) channels [19].

detector efficiencies, resolution effects and biases. The data are corrected using the following expression

$$\vec{N}_{part} = \vec{f}_{part!reco} \cdot \mathbf{M}_{part}^{reco} \cdot \vec{f}_{reco!part} \cdot \vec{f}_{accpt} \cdot \left(\vec{N}_{reco} - \vec{f}_{bkg} \right), \tag{4}$$

where $\vec{f}_{accpt}$ is an acceptance correction for all selection efficiencies except for the jet multiplicity requirement; $\vec{f}_{reco!part}$ is a correction for events passing the jet multiplicity requirement at reconstruction level but not at particle level; $\mathbf{M}_{part}^{reco}$ is a response matrix provided for the unfolding of the jet multiplicity to correct for the jet resolution and reconstruction effects. Finally, $\vec{f}_{part!reco}$ corrects for events which fulfill the particle-level jet multiplicity requirement but fail the same at reconstruction level. Fig. 6 shows the fully corrected particle-jet multiplicities for various jet transverse momentum thresholds in the electron channel compared to different theoretical predictions. For the lowest jet transverse momentum threshold, all predictions agree with data in the three- and four-jet bins. MC@NLO underestimates data for events with more than six jets in the lowest jet transverse momentum bin and for lower multiplicities as the

transverse momentum threshold increases.

CMS provides the normalised differential cross-section of $t\bar{t}$ events as a function of the number of additional partons, which are defined as those with transverse momenta larger than 30 GeV and whose distance ΔR to all $t\bar{t}$ decay products is larger than 0.5. Fig. 7 shows this distribution compared with expectations from different generators. The measured fractions of events with zero, one and two or more additional hard partons are in excellent agreement with MadGraph and Powheg generators. Furthermore, already with the 7 TeV dataset, the precision of the measurement is significantly better than the scale variations and can be used to constrain them.

5   Summary

$t\bar{t}$ jet multiplicity measurements are useful to test theoretical predictions and to look for beyond the Standard Model signals. Both ATLAS and CMS find good agreement between data and simulation except for MC@NLO Monte Carlo, which produces too little jet activity at high jet multiplicities. Furthermore, there is some indication that data prefer a lower α_S value for multi-leg generators. Finally, with the present data sets, the ability to constrain models at large jet multiplicities is limited by the large statistical uncertainty.

References

[1] G. Aad *et al.* [ATLAS Collaboration], JINST **3** (2008) S08003.

[2] S. Chatrchyan *et al.* [CMS Collaboration], JINST **3** (2008) S08004.

[3] M. Cacciari, G. P. Salam and G. Soyez, JHEP **0804** (2008) 063, arXiv:0802.1189 [hep-ph].

[4] M. L. Mangano, M. Moretti, F. Piccinini, R. Pittau and A. D. Polosa, JHEP **0307** (2003) 001, hep-ph/0206293.

[5] G. Corcella, I. G. Knowles, G. Marchesini, S. Moretti, K. Odagiri, P. Richardson, M. H. Seymour and B. R. Webber, JHEP **0101** (2001) 010, hep-ph/0011363.

[6] J. Alwall, M. Herquet, F. Maltoni, O. Mattelaer and T. Stelzer, JHEP **1106** (2011) 128, arXiv:1106.0522 [hep-ph].

[7] T. Sjostrand, S. Mrenna and P. Z. Skands, JHEP **0605** (2006) 026, hep-ph/0603175.

[8] S. Frixione, P. Nason and C. Oleari, JHEP **0711** (2007) 070, arXiv:0709.2092 [hep-ph].

[9] S. Frixione and B. R. Webber, JHEP **0206** (2002) 029, hep-ph/0204244.

[10] B. P. Kersevan and E. Richter-Was, hep-ph/0405247.

[11] M. Aliev, H. Lacker, U. Langenfeld, S. Moch, P. Uwer and M. Wiedermann, Comput. Phys. Commun. **182** (2011) 1034, arXiv:1007.1327 [hep-ph].

[12] N. Kidonakis, Phys. Rev. D **82** (2010) 114030, arXiv:1009.4935 [hep-ph].

[13] G. Aad *et al.* [ATLAS Collaboration], Eur. Phys. J. C **72** (2012) 2043, arXiv:1203.5015 [hep-ex].

[14] CMS Collaboration, CMS-PAS-TOP-12-023.

[15] CMS Collaboration [CMS Collaboration], CMS-PAS-TOP-12-041.

[16] A. Hocker and V. Kartvelishvili, Nucl. Instrum. Meth. A **372** (1996) 469, hep-ph/9509307.

[17] V. Blobel, hep-ex/0208022.

[18] ATLAS Collaboration, ATLAS-CONF-2012-155.

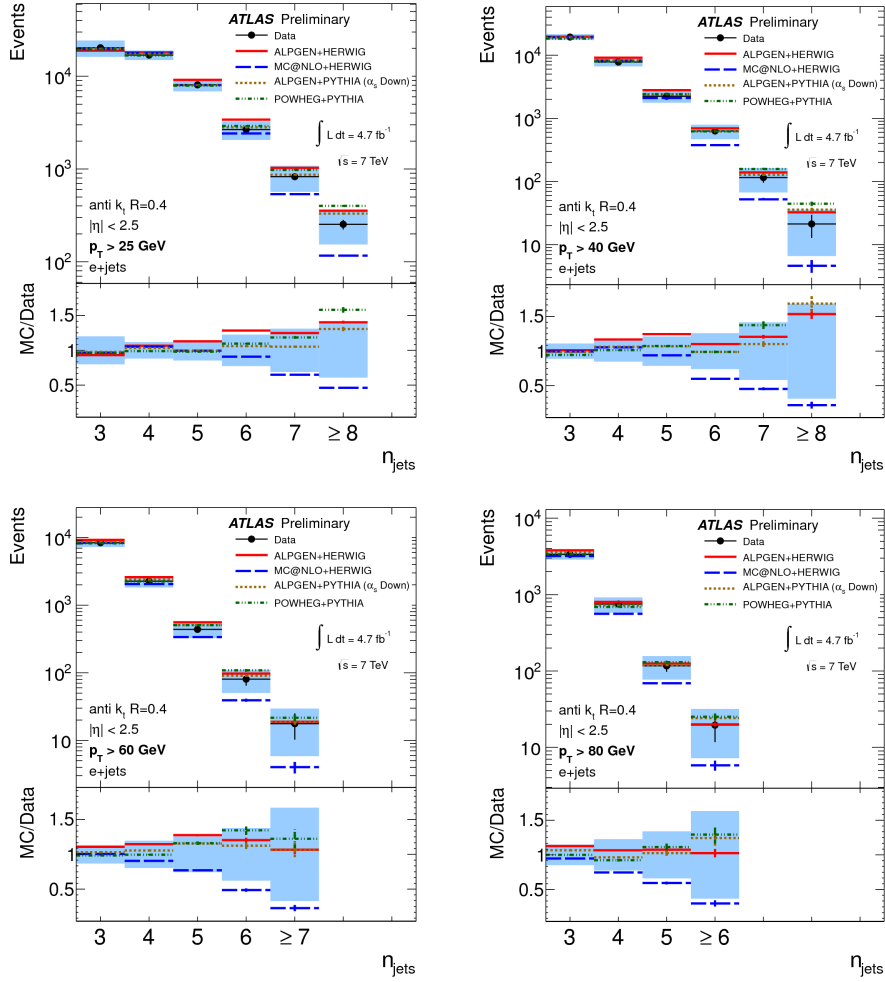[19] CMS Collaboration, CMS-PAS-TOP-12-018.

Figure 6: ATLAS particle-jet multiplicities for the electron channel and the jet p_T thresholds (from left to right and top to bottom) 25, 40, 60 and 80 GeV. Data are shown in comparison to several theoretical predictions [18].
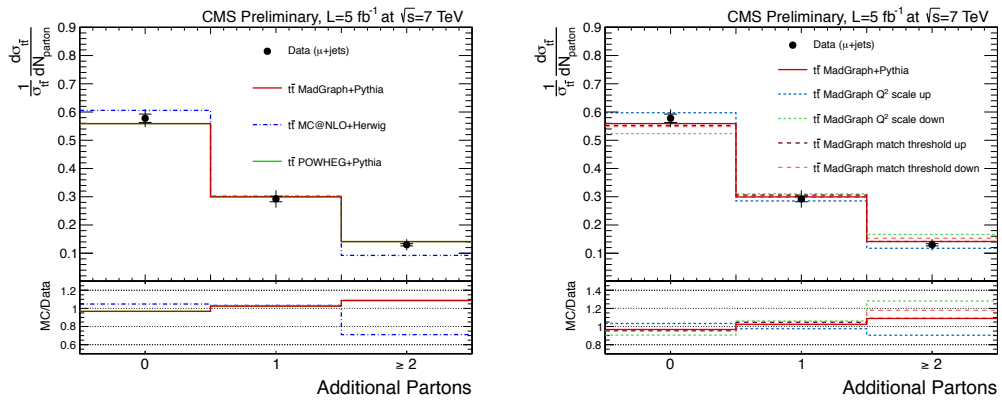
Figure 7: Measured CMS normalised cross-section measurement of $t\bar{t}$ processes with additional partons in the μ+jets channel [19].